Acta Montanistica Slovaca
ISSN 1335-1788
actamont.tuke.sk

Multispectral Discrimination of Mangroves of the Indian Sundarban Using Machine Learning Techniques

Sourav BHATTACHARYYA[1,2] *and Nilanchal PATEL*[1*]

Authors' affiliations and addresses:
[1] Department of Remote Sensing and Geoinformatics, Birla Institute of Technology, Mesra, Ranchi, Jharkhand, PIN 835215, India
e-mail: sourav16787@gmail.com

[2] Faculty, Department of Earth Science and Remote Sensing, JIS University, 81 Nilgunj Road, Agarpara, Kolkata-700109, West Bengal, India

***Correspondence:**
Nilanchal Patel, Faculty, Department of Remote Sensing and Geoinformatics, Birla Institute of Technology, Mesra, Ranchi,
Jharkhand, PIN 835215, India
e-mail: npatel@bitmesra.ac.in

Acknowledgement:
The authors acknowledge the Birla Institute of Technology,Mesra,Ranchi,India,for permitting them to perform the desired research.

How to cite this article:
Bhattacharyya, S. and Patel, N. (2025), Multispectral Discrimination of Mangroves of Indian Sundarban Using Machine Learning Techniques. *Acta Montanistica Slovaca*, Volume 30 (4), 1034-1047

DOI:
https://doi.org/10.46544/AMS.v30i4.14

Abstract
Mangroves in the Indian Sundarban are crucial to maintaining ecological balance and require precise monitoring to address land-cover changes and vegetation health under dynamic climatic conditions. This study utilizes LANDSAT-8/9 OLI imagery and three machine learning classifiers, viz. Maximum Likelihood (ML), Support Vector Machine (SVM), and Spectral Angle Mapper (SAM), to delineate mangroves and other LULC during the pre- and post-monsoon seasons. Pre-monsoon image analysis showed more precise spectral discrimination than post-monsoon satellite data. The post-monsoon period is characterized by increased river flow, and green vegetation and crops, resulting in identical between-class spectral signatures. In contrast, exposed mudflats, dry agricultural lands, and shallow rivers improved between-class discrimination in the pre-monsoon period. ML demonstrated better performance across both seasons, achieving high mangrove accuracy (>95%), robust Kappa values (0.96 pre-monsoon, 0.94 post-monsoon), and AUC scores (0.98 and 0.96), followed by SVM. At the same time, SAM suffered significantly during the post-monsoon period due to substantial between-class spectral similarity. Seasonal water level fluctuations, changes in settlement with vegetation, and agricultural activities influenced LULC mapping. The AUC-ROC curve further validated the classifiers' efficiency. By selecting three contrasting classifiers and explicitly accounting for the limitations of Landsat-8/9 OLI data, this study provides a rigorous benchmark for evaluating classifier robustness under seasonal variability in Sundarbans.
The research revealed the superiority of the traditional maximum likelihood classifier over SVM and SAM in both seasons. Further, it provides critical insights into the seasonal dynamics of mangrove ecosystems, the need for improved LULC mapping, and the conservation and management of mangroves.

Keywords
Machine Learning Classifiers; Mangroves; LANDSAT-OLI; AUC-ROC Curve; LULC

Introduction

Mangroves are critical ecosystems that provide essential ecosystem services, including carbon sequestration, coastal protection, and biodiversity conservation. The Indian Sundarbans, a UNESCO World Heritage Site, is the largest contiguous mangrove forest globally and a vital ecological hotspot (Giri et al., 2007). However, these ecosystems are increasingly threatened by climate change, sea-level rise, and anthropogenic activities such as deforestation and the expansion of aquaculture. Effective conservation of this fragile ecosystem requires precise monitoring of land-use and land-cover (LULC) changes and vegetation health. Recent advancements in remote sensing and machine learning offer powerful tools for analyzing spatiotemporal dynamics, enabling robust monitoring of mangrove ecosystems and sustainable management.

Several studies have demonstrated the potential of integrating remote sensing and machine learning for mangrove monitoring. Maximum Likelihood Classification (MLC) and NDVI indices were employed to map mangrove vegetation in Taiwan, emphasizing the importance of spectral separability (Lee and Yeh, 2009). An MLC program was applied to distinguish mangrove and non-mangrove areas, revealing that mangrove habitats expanded by 15.18 and 40 hectares at monitoring sites over ten years. Additionally, the study demonstrated that satellite imagery could effectively differentiate mangroves from other vegetation types, addressing challenges in monitoring inaccessible areas and evaluating long-term vegetation changes using remote sensing techniques. Machine learning classifiers, such as CART and Random Forest (RF), were applied to detect changes in mangrove cover along the Mumbai coast (Sawant et al., 2024). These methods demonstrated the ability to handle complex datasets with high-dimensional features, offering robust classification outcomes across varying timeframes. Maximum Likelihood (ML) demonstrated statistical robustness in modeling class probabilities, making it effective for datasets with clear spectral separability (Ahmad and Quegan, 2012). Similarly, Support Vector Machine (SVM) successfully handled high-dimensional feature spaces by utilizing kernel functions to efficiently classify non-linear data (Sun et al., 2019). These approaches collectively highlight the potential of advanced classification methods in achieving reliable LULC outcomes. Random Forest (RF) and ANN were employed to analyze mangrove distributions in the Red Sea, resulting in significant improvements in landscape connectivity (Bindajam et al., 2023). Sentinel-2 imagery was analyzed for national-scale mangrove species mapping in China, achieving high classification accuracy (Zhao et al., 2024). This study demonstrated the effectiveness of combining high-resolution multispectral data with advanced machine-learning algorithms to differentiate mangrove species across diverse environmental conditions.

Additionally, Sentinel-2's fine spatial and temporal resolutions proved crucial for capturing seasonal variations and improving classification outcomes.However, few studies focus on mangroves in the Sundarbans, especially in assessing seasonal variations and their impact on classification performance.While significant progress has been made in mangrove monitoring using various machine learning and remote sensing techniques in regions such as Taiwan, Mumbai, the Red Sea, and coastal China, there is a lack of a systematic examination of seasonal influences on classification performance, specifically in the Sundarbans, an ecologically fragile and dynamic system. Previous research has often focused on single-season mapping or utilized higher-resolution datasets without explicitly addressing the impact of hydrological variability and monsoonal cycles on spectral separability. This study aims to bridge that gap by integrating Landsat-8/9 OLI imagery with three distinct classifiers (ML, SVM, and SAM) and assessing their performance using accuracy metrics and AUC-ROC analysis across both pre- and post-monsoon seasons, thereby providing new insights into the spatiotemporal reliability of the classifiers. A seasonal comparative approach will enhance methodological understanding and yield practical implications for long-term mangrove monitoring and conservation planning in the Sundarbans, where climate variability and anthropogenic pressures necessitate precise, adaptable classification strategies. Though Landsat-OLI has moderate spatial resolution and extensive temporal coverage, it is widely utilized for mangrove monitoring and LULC classification (Islam et al., 2019). This is because it can capture long-term trends and seasonal variations, making it an essential dataset for understanding ecosystem dynamics and complementing datasets like Sentinel-2.

Pre-monsoon conditions, with high salinity, exposed mudflats, and dry croplands, provide clearer spectral separability, whereas the post-monsoon image reflects denser, greener vegetation and cropswith overlapping spectral signatures (Small and Sousa, 2024). Comparative seasonal analysis reveals the effect of the varying environmental conditions on the classification efficiency of the different classifiers.

The specific objectives of this research include (1) discriminating Sundarban mangroves using Landsat-OLI images in pre- and post-monsoon seasons, (2) comparing different machine learning techniques in terms of classification accuracy, and (3) evaluating classifier performance using the AUC-ROC curve to identify the most suitable technique for mangrove delineation. The results of this research will improve the monitoring and sustainable management of the Sundarbans mangroves, offering valuable insights into their conservation amid increasing environmental concerns and climate change.

Study area

The Indian Sundarban mangroves in the northern Bay of Bengal are ecologically and geographically significant because they lie at the confluence of nutrient-rich rivers and tidal waterways, supporting diverse flora and fauna. It also offers vital ecological services and livelihoods. The region spans six administrative blocks in North 24 Parganas and 13 blocks in South 24 Parganas districts of West Bengal, demarcated between 21°32′N to 22°40′N latitude and 88°05′E to 89°00′E longitude (Fig. 1). Its boundaries are defined by the Hooghly River in the west, Bay of Bengal in the south, and Ichamati-Kalindi-Raimongal Rivers in the east. This low-lying delta, formed 10,000–3,000 years ago, features salt marshes, mangrove swamps, and intricate drainage systems. Receiving 180–200 cm of annual rainfall, the area is prone to cyclones and storm surges, leading to frequent flooding.There are 25 truemangrove species and 30 mangrove associates in the Indian Sundarban (Ghosh et al., 2002).

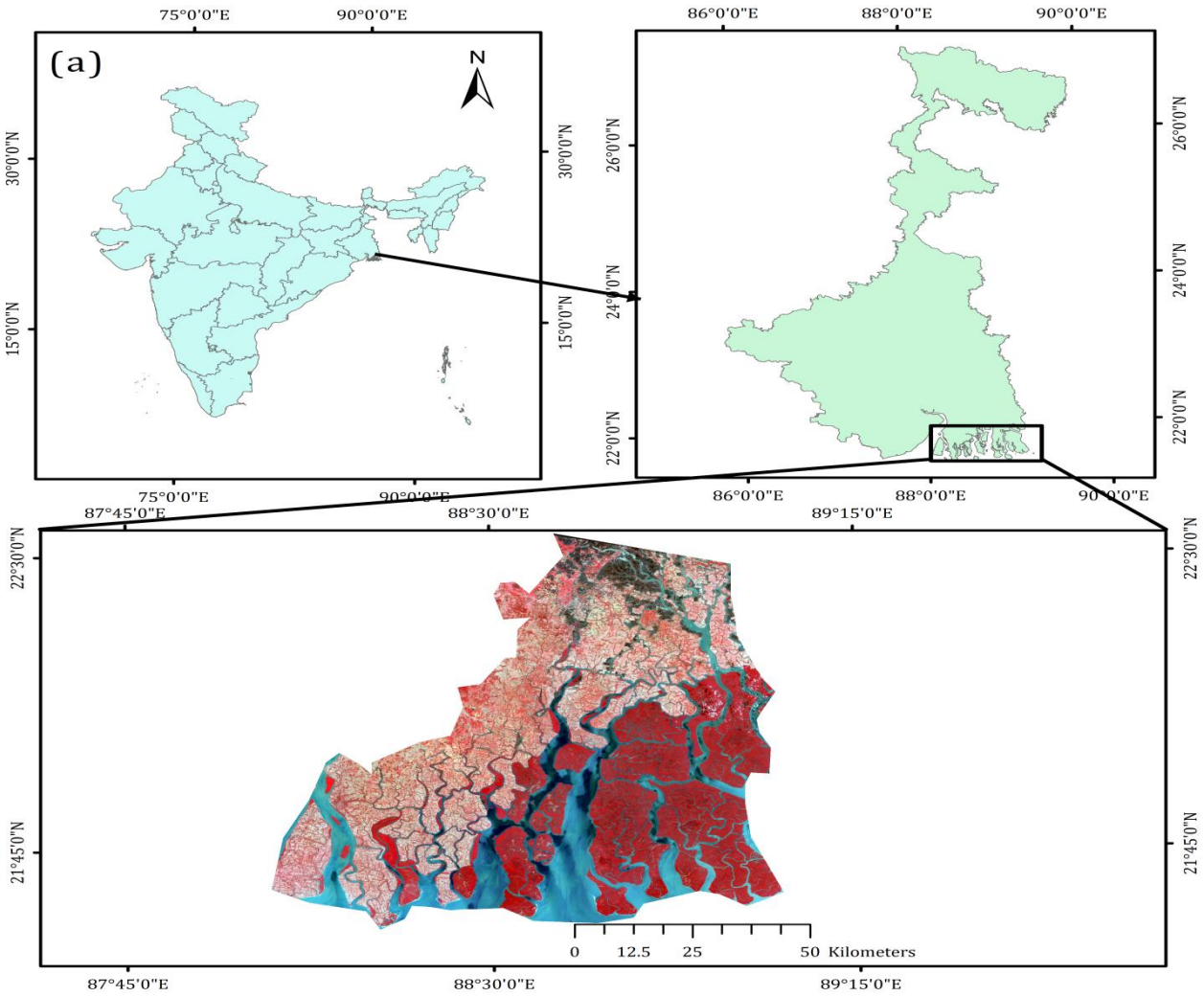

Fig. 1: Study Area

Materials and Methods

Data Acquisition and Preprocessing

This study utilized Landsat-8 and Landsat-9 Operational Land Imager (OLI) datasets for seasonal LULC monitoring in the Indian Sundarbans (Fig. 2). The datasets were acquired for pre-monsoon (April 25, 2024) and post-monsoon (November 25, 2023) periods (Table 1). The spatial resolution for multispectral bands is 30 meters. The temporal resolution of the imagery is 16 days, ensuring frequent observations for temporal analysis. The radiometric resolutions of 12 bits for Landsat-8 and 14 bits for Landsat-9 enable enhanced spectral discrimination among LULC categories.Level-2 data products were used to perform classification (USGS, 2023).

Methodology Flow Chart

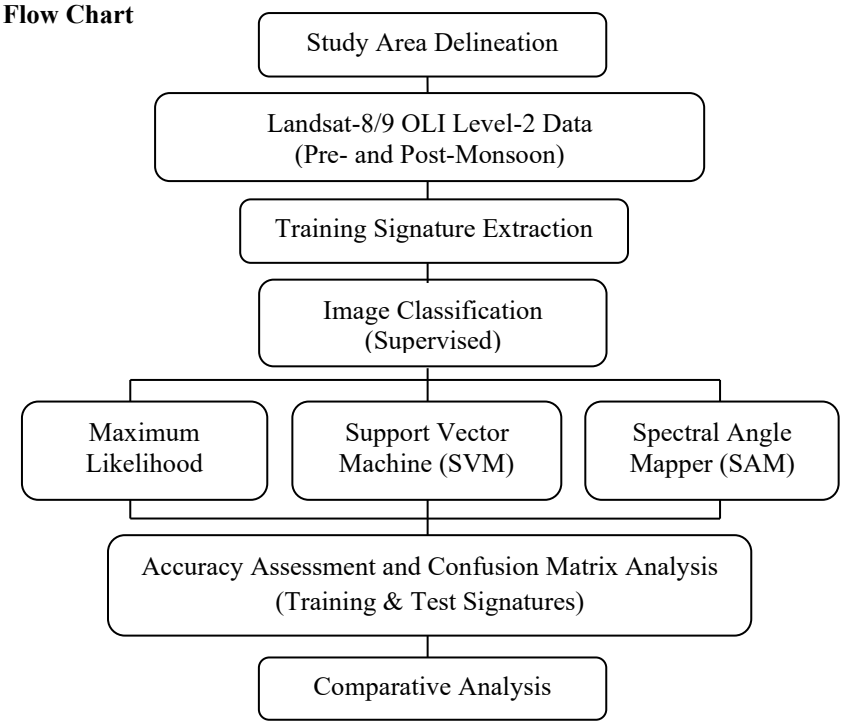

Table 1. Satellite Data

Season	Data Source	Date	Spatial Resolution	Radiometric Resolution	Temporal Resolution
Pre-Monsoon	Landsat-9 OLI	April 25, 2024	30 m (multispectral), 15 m (panchromatic)	14-bit	16 days
Post-Monsoon	Landsat-8 OLI	November 25, 2023	30 m (multispectral), 15 m (panchromatic)	12-bit	16 days

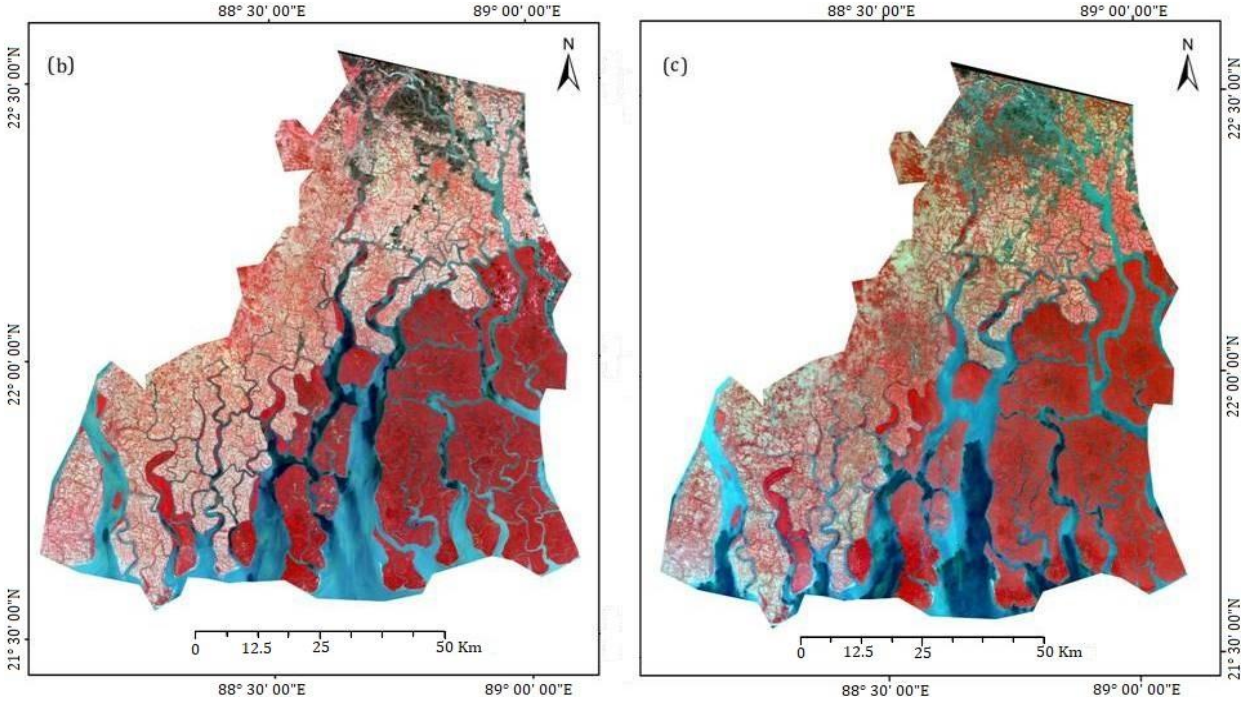

Fig. 2: Landsat- OLI (b) L9 of April 25 2024 and (c) L8 of November 25 2023

Software and Data Used

The study employed ERDAS Imagine 2022® for shapefile preparation, supervised classification, and .aoi file generation. ArcMap 10.8® was utilized for accuracy assessment through a confusion matrix and SVM classification. Python libraries such as scikit-learn, matplotlib, and numpy were used in a Jupyter Notebook to evaluate classifier performance and plot AUC-ROC curves (Rajamani and Iyer, 2023).

Study Area Delineation and Training Data Preparation

The spatial extent of the study was delineated using a shapefile representing the Indian Sundarbans mangrove ecosystemwith reference to the Bhuvan map (2018-23) obtained from ISRO's geoportal. Training data for supervised classification were created using region-specific knowledge and visual interpretation in ERDAS Imagine (.aoi files). Test data points for validation were compiled as an accuracy_points.shp file in ArcMap 10.8. The Sundarbans region was chosen for its ecological significance and vulnerability to anthropogenic pressures and climate change (Sen, 2019).

Supervised classification and accuracy assessment

LULC classification was performed employing maximum likelihood (ML), support vector machine (SVM), and spectral angle mapper (SAM)classifiers(Table 2). Accuracy assessments were conducted using confusion matrices, kappa coefficients, and overall accuracy metrics. Additionally, the AUC-ROC curves were plotted to compare classifier performance.

1. Maximum Likelihood (ML): Confusion matrices were generated using ArcMap (Fig. 3).

2. Support Vector Machine (SVM): Classification and contingency matrix generation were performed in ArcMap (Fig. 4).

3. Spectral Angle Mapper (SAM): Error matrices were validated using both ERDAS Imagine and ArcMap (Fig. 5) (Kruse et al., 1993).

4. Rationale and Data Limitations: The inclusion of these three classifiers enabled benchmarking across fundamentally different methodologies. Maximum Likelihood (ML), Support Vector Machine (SVM), and Spectral Angle Mapper (SAM) were selected because they represent distinct classification approaches, allowing a robust comparative evaluation among three classifiers. ML is a parametric technique that yields statistically reliable results when spectral separability is high; SVM is a nonparametric machine learning algorithm that effectively handles complex, high-dimensional data. SAM, which relies on spectral similarity, offers a simpler yet more sensitive approach to spectral variability, making it a useful benchmark. While Landsat-8/9 OLI provides consistent temporal coverage and moderate resolution suitable for regional analysis, the data do have limitations. Cloud cover, seasonal spectral noise from vegetation and hydrological changes, and the 30 m spatial resolution may affect classification accuracy. These issues were mitigated through cloud-free, atmospherically corrected Level-2 products and independent accuracy validation. However, future studies should consider higher-resolution datasets and multi-sensor integration to minimise these uncertainties.

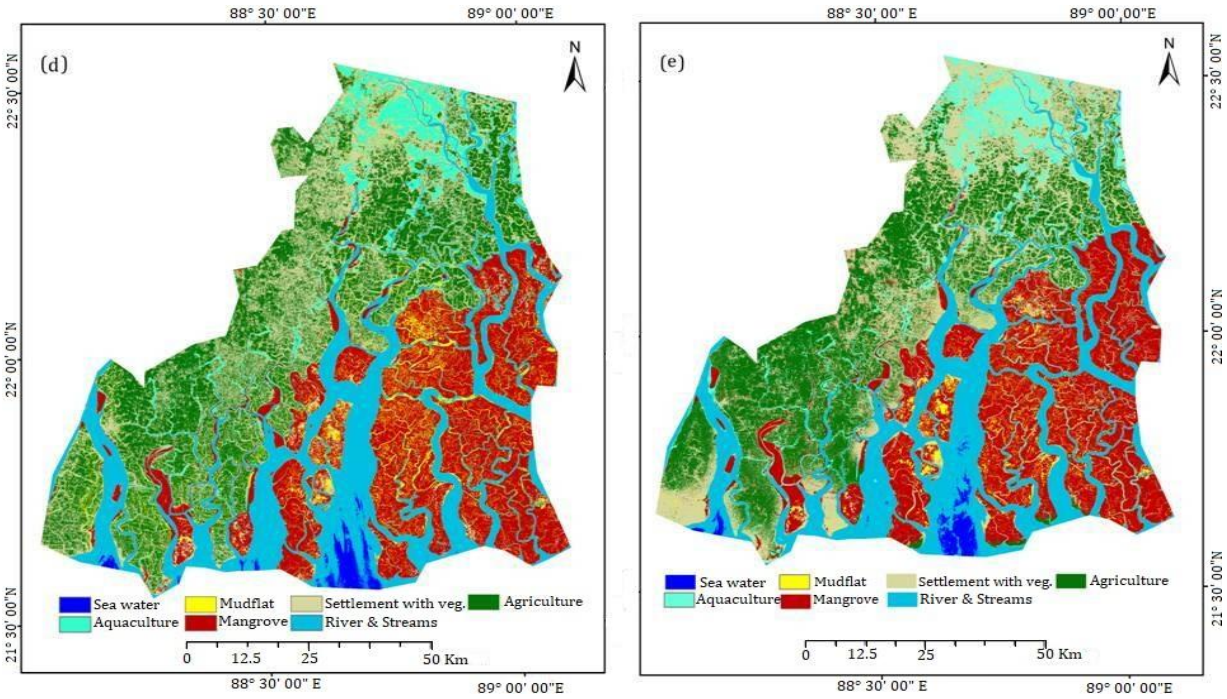

Fig. 3: Classified Image of (d) April 25 2024 and (e) November 25 2023 with Maximum Likelihood (ML)

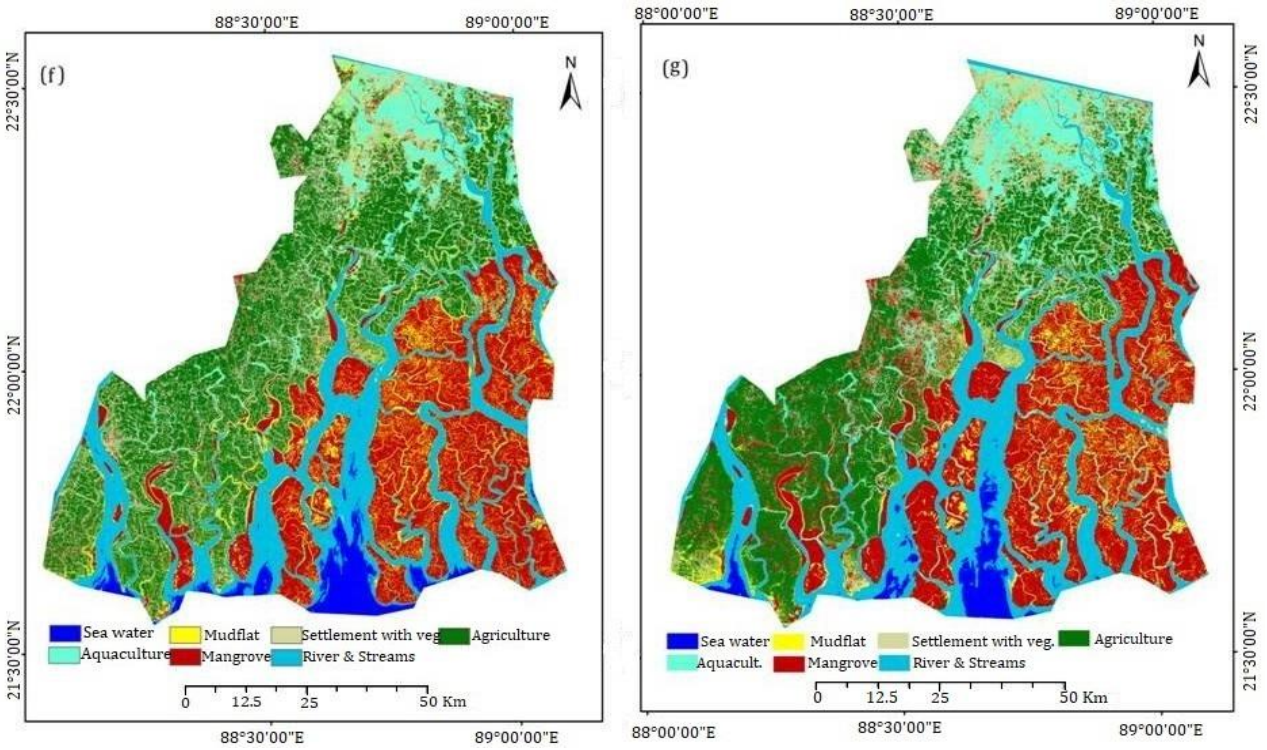

Fig. 4: Classified Image of (f) April 25 2024 and (g) November 25 2023 with Support Vector Machine (SVM)

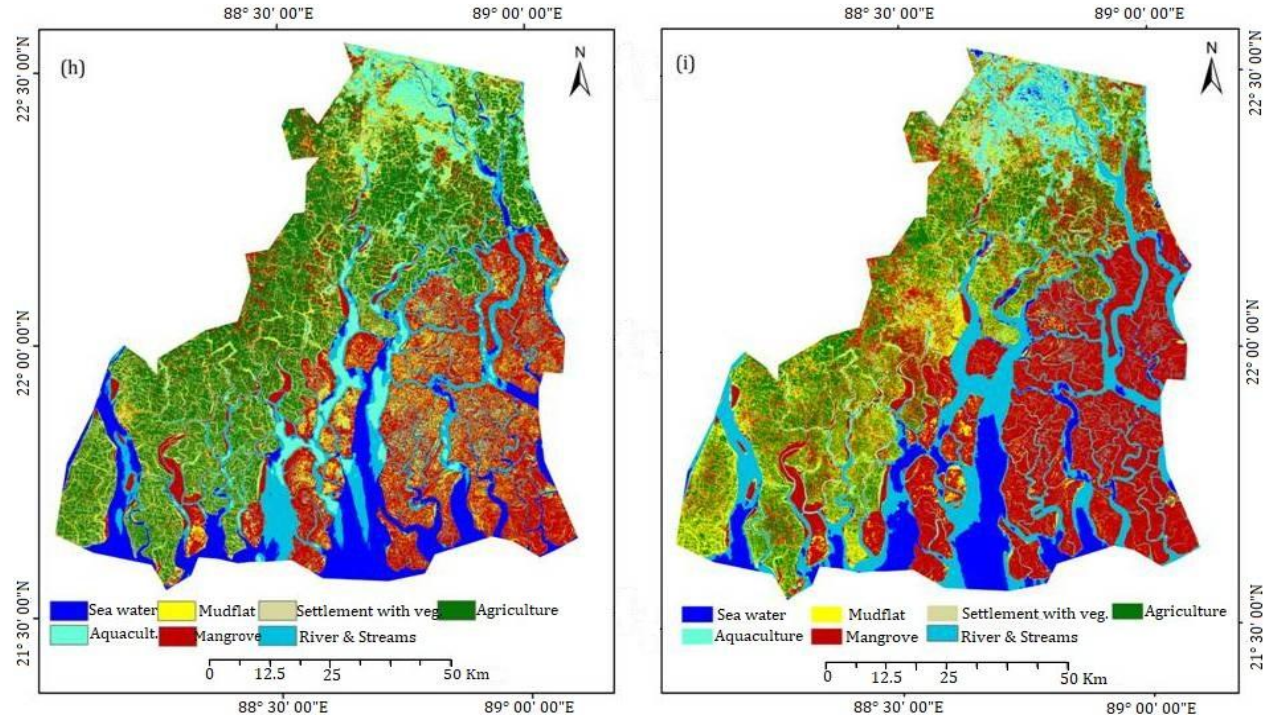

Fig. 5: Classified Image of (h) April 25 2024 and (i) November 25 2023 with Spectral Angle Mapper (SAM)

Table 2. Accuracy Metrics

Matrix	Formula	Description	Reference
User's Accuracy (UA)	$\frac{x_{ii}}{x1+}$	x_{ii} is correctly classified pixels for a class, and x_{1+} is the total pixels classified in that class	Jensen et al., 1996

Producer's Accuracy (PA)	$\frac{x_{jj}}{x+j}$	x_{jj} is the correctly classified pixels for a class, and x_{+j} is the training pixels for the particular class	Jensen et al., 1996
Overall Accuracy (OA)	$\frac{\sum P_{ii}}{N}$	P_{ii} is the total correctly classified pixels, and N is the total number of pixels taken.	
kappa Accuracy	$\kappa = \frac{N\sum_{i=1}^{r} x_{ii} - \sum_{i=1}^{r}(xi_{+} \times x_{+i})}{N^2 - \sum_{i=1}^{r}(xi_{+} \times x_{+i})}$	N is the total number of observations (sum of all elements in the confusion matrix); x_{ii}: The diagonal elements of the confusion matrix, representing the number of observations where the predicted class matches the actual class (correctly classified instances for class i); $\sum_{i=1}^{r} x_{ii}$ is the sum of the diagonal elements, representing the total number of correctly classified observations; x_{i+}: Sum of the i-th row of the confusion matrix, representing the total number of observations predicted as class i; x_{+i}: sum of the i -th column of the confusion matrix, representing the total number of observations that actually belong to class i. $\sum_{i=1}^{r}(xi_{+} \times x_{+i})$ is the expected number of agreements by chance, calculated based on the row and column totals of the confusion matrix. r is the total number of classes in the confusion matrix.	Jensen et al., 1996
Maximum Likelihood (ML)	$g_i(x) = \sum_{i=1}^{r} \ln P(\omega i) - \frac{1}{2}\sum_{i=1}^{r} \ln \lvert \sum_i \rvert - \frac{1}{2}\sum_{i=1}^{r}[(x-\mu i]\, T \sum \bar{i}^{1}(x-\mu i)]$	r: Number of classes. First term: Prior probability of belonging to a class. Second term: Penalty term based on the covariance (spread) of the class. Third term: Mahalanobis distance from the feature vector x to the mean of the class, scaled by covariance.	
Spectral Angle Mapper (SAM)	$\theta = \cos^{-1}\left(\frac{X.R}{\lvert\lvert X\rvert\rvert\, \lvert\lvert R\rvert\rvert}\right)$	θ: Spectral Angle; $X.R$: Dot product of the pixel spectrum X and reference spectrum R; $\lvert\lvert X\rvert\rvert$: Magnitude (norm) of the vector X, calculated as: $\lvert\lvert X\rvert\rvert = \sqrt{\sum_{i=1}^{n} X_i{}^2}$. $\lvert\lvert R\rvert\rvert$: Magnitude (norm) of the vector R, calculated similarly.	Liu and Yang ,2013
Support Vector Machine (SVM)	Linear: $\min_{\omega,b} \frac{1}{2}\lvert\lvert\omega\rvert\rvert^2$, subject to $y_i(\omega^T x_i + b) \geq 1 \forall i$ Soft Margin: $\min_{\omega,b,\zeta} \frac{1}{2}\lvert\lvert\omega\rvert\rvert^2 + C\sum_{i=1}^{N}\zeta_i$ subject to $y_i(\omega^T x_i + b) \geq 1 - \zeta_i \forall i$	ω: Weight vector (normal to the hyperplane); b: Bias term; x_i : Feature vector for the i-th data point; y_i: Class label for the i-th data point (+1 or −1); $\lvert\lvert\omega\rvert\rvert^2$: Magnitude of the weight vector. ζ_i: Slack variable for the i-th data point (penalty for misclassification). C: Regularization parameter controlling the trade-off between margin size and classification error.	Keerthi et al., 2005

Results and Discussion

Output Images

The classified images for the pre-monsoon (April 25, 2024) and post-monsoon (November 25, 2023) datasets were evaluated using test pixels. For the pre-monsoon dataset, mangrove vegetation achieved a Producer's Accuracy of 99.01%, aquatic areas 95.95%, and settlements 97.33% using the ML classifier (Table 3). In the post-monsoon dataset, mangrove vegetation's Producer's Accuracy decreased to 96.63% (Table 4),and aquatic areas achieved 87.65% accuracy (Table 5). SVM yielded Overall Accuracies of 85.67% and 84.7% for pre- and post-monsoon datasets, respectively. SAM demonstrated lower accuracies of 74.49% for the pre-monsoon dataset and 71.02% for the post-monsoon dataset (Table 6). These seasonal variations could be attributed to the changes in LULC classes influenced by hydrological and ecological conditions (Sen, 2019).

Table 3. Accuracy Matrix (in %) of Test Pixels of the Classified Image (LANDSAT 9, APRIL 25 2024) - ML Classifier

LULC	AG	AQ	SV	MG	MF	RS	SW	Row Total	UA
AG	98.35	0	0.8	0	0	0	0	3418	99.62
AQ	0.06	96.55	0.6	0.06	0	2.42	0	2431	79.43
SV	1.56	3.25	98.27	0.89	3	0	0	1814	81.26
MG	0	0	0	99.01	0	0	0	21207	100
MF	0.03	0	0.33	0.03	97	0	0	984	98.68

RS	0	0.2	0	0	0	95.95	2.67	19138	98.88
SW	0	0	0	0	0	1.63	97.33	8005	96.00
Column Total	3462	2000	1500	21418	1001	19721	7895	56997	

Table 4. Accuracy Matrix (in %) of Test Pixels of the Classified Image (LANDSAT 8, November 25, 2023) - SVM Classifier

ClassValue	SW	RS	MG	MF	AG	SV	AQ	Row Total	UA
SW	10	0	0	0	0	0	0	10	100
RS	0	62	0	0	0	0	1	63	98.41
MG	0	0	86	0	5	3	0	94	91.49
MF	0	0	1	15	1	4	2	23	65.22
AG	0	0	2	0	81	3	0	86	94.19
SV	0	3	0	1	14	22	3	43	51.16
AQ	0	6	0	0	4	1	23	34	67.65
Column Total	10	71	89	16	105	33	29	353	0
PA	100	87.32	96.63	93.75	77.14	66.67	79.31	0	84.70

Table 5. Accuracy Matrix (in %) of Test Pixels of the Classified Image (LANDSAT 8, November 25, 2023) - ML Classifier

LULC	SW	MF	SV	AG	AQ	MG	RS	Row Total	UA
SW	10	0	0	0	0	0	0	10	100
MF	0	8	1	0	1	0	0	10	80.00
SV	0	0	36	28	4	7	5	80	45.00
AG	0	0	2	73	0	3	0	78	93.59
AQ	0	0	0	2	17	0	5	24	70.83
MG	0	0	0	0	0	83	0	83	100
RS	0	0	0	0	0	0	71	71	100
Column Total	10	8	39	103	22	93	81	356	0
PA	100	100	92.31	70.87	77.27	89.25	87.65	0	83.71

Table 6. Overall Accuracy (in %) of Test Pixels of Classified Images

% Overall Accuracy	SAM	SVM	ML
Pre-Monsoon (April)	74.49	85.67	97.54
Post-Monsoon (November)	71.02	84.70	83.71

Classification Accuracy: Test Data

The analysis used Level-2 data, preprocessed for radiometric, geometric, and atmospheric corrections, ensuring high-quality datasets ready for classification and analysis. Over the Indian Sundarban, Landsat satellites pass at 10:30 AM local time (descending orbit) to capture images for seasonal analysis.

For the pre-monsoon dataset (April 2024), the ML classifier achieved an Overall Accuracy of 97.54% and a Kappa Coefficient of 0.96 for test data (Tables6 and 7). The SVM classifier demonstrated an Overall Accuracy of 85.67% with a Kappa Coefficient of 0.82, while SAM achieved 74.49% accuracy and a Kappa Coefficient of 0.69 (Tables6 and 7). In the post-monsoon dataset (November 2023), ML achieved an Overall Accuracy of 83.71% with a Kappa Coefficient of 0.80. SVM performed well with an accuracy of 84.7% and a Kappa Coefficient of 0.81, while SAM's accuracy reduced to 71.02% with a Kappa Coefficient of 0.64. The consistent performance of ML and SVM underscores their reliability for LULC classification in diverse seasonal conditions (Belgiu and Drăguţ, 2016).

The comparison of classifiers shows differences in accuracy and the reasons underlying their performance. The ML classifier consistently outperformed others because its probabilistic framework leverages class variance and covariance. This makes it well-suited to datasets with clearer spectral separability, like in the pre-monsoon, when exposed mudflats and dry croplands enhance contrast. SVM produced stable results in both seasons, which

reflects its ability to handle non-linear and high-dimensional feature spaces. This strength enabled it to partially address spectral overlaps during post-monsoon greening, when agricultural fields and mangroves appeared spectrally similar. In contrast, SAM relies only on angular similarity between spectral signatures, making it less effective in those conditions and leading to misclassifications in post-monsoon imagery.

These differences have direct practical implications for mangrove monitoring. The consistent superiority of ML confirms its suitability as a baseline classifier for operational monitoring programs that use medium-resolution imagery. The relative robustness of SVMs shows that they are valuable in dynamic ecosystems like the Sundarbans, where spectral confusion from seasonal flooding and vegetation growth is common. On the other hand, the poor performance of SAM suggests it is less suitable for diverse tropical environments. Using season-specific strategies, such as prioritising pre-monsoon imagery to improve separability, can further improve monitoring results. These insights offer conservation practitioners and policymakers clear guidance on selecting reliable classifiers to monitor mangrove health and land-use changes across different seasons.

Table 7. Kappa Accuracy (κ) of Test Pixels of Classified Images

Kappa Accuracy	SAM	SVM	ML
Pre-Monsoon(April)	0.69	0.82	0.96
Post-Monsoon(November)	0.64	0.81	0.80

AUC-ROC Analysis of Classifiers

The AUC-ROC curves were determined to quantify classifier performance for both seasons. For the pre-monsoon dataset, the ML classifier achieved an AUC of 0.98, SVM 0.82, and SAM 0.69 (Table 8). For the post-monsoon dataset, ML achieved an AUC of 0.96, SVM 0.81, and SAM 0.64. These values indicate that ML outperforms SVM in distinguishing LULC classes, followed by SAM, which exhibits the least efficiency. The high AUC values for ML indicate its robustness in mitigating spectral overlap effects, particularly in mangrove regions (Heumann, 2011).

Table 8. Pre-monsoon (April) and Post-monsoon (November) AUC of Classified Images

Classifier	AUC (April)	Performance	AUC (November)	Performance
ML	0.98	Outstanding	0.96	Outstanding
SAM	0.69	Acceptable	0.64	Poor
SVM	0.82	Excellent	0.81	Excellent

The study critically examines the role of seasonal dynamics in classifying land use and land cover (LULC) in the Indian Sundarbans using Landsat OLI data and advanced machine learning techniques. Seasonal variations significantly impact classification performance, with pre-monsoon conditions characterized by high salinity and exposed mudflats, enabling better spectral separability than the spectral similarities of the post-monsoon season (Chopra et al., 2001). These variations were evident in the classifiers used in this study: Maximum Likelihood (ML), Support Vector Machine (SVM), and Spectral Angle Mapper (SAM). ML consistently outperformed other classifiers across both seasons, achieving an overall accuracy of 97.54% and a kappa coefficient of 0.96 during the pre-monsoon season. It demonstrated producers' accuracies (PAs) of 99.01% for mangroves and 97.33% for seawater. SVM followed, achieving 85.67% overall accuracy and a kappa coefficient of 0.82, with high PA values for mangroves (89.13%) and seawater (100%) (Fig. 6). SAM, however, showed relatively poor performance, achieving 74.49% overall accuracy and a kappa coefficient of 0.69, reflecting its sensitivity to spectral variability.

In the post-monsoon dataset, increased vegetation density and overlapping spectral signatures posed greater challenges for classification (Deval and Joshi, 2022). ML maintained its superior performance, followed by SVM, achieving an overall accuracy of 84.70% and a kappa coefficient of 0.81, with a PA of 96.63% for mangroves. SAM's performance further declined, signifying its limitations in distinguishing between overlapping spectral signatures. These results align with previous studies that emphasized the efficacy of machine learning classifiers for mangrove ecosystem monitoring. For instance, RF and ANN have already been used to analyze mangrove distributions, improving landscape connectivity and classification accuracy (Ahmad and Quegan, 2012). Similarly, CART and Random Forest were used to detect changes in mangrove cover along the Mumbai coast, demonstrating their reliability for temporal analysis (Baviskar and Dhiman, 2022).

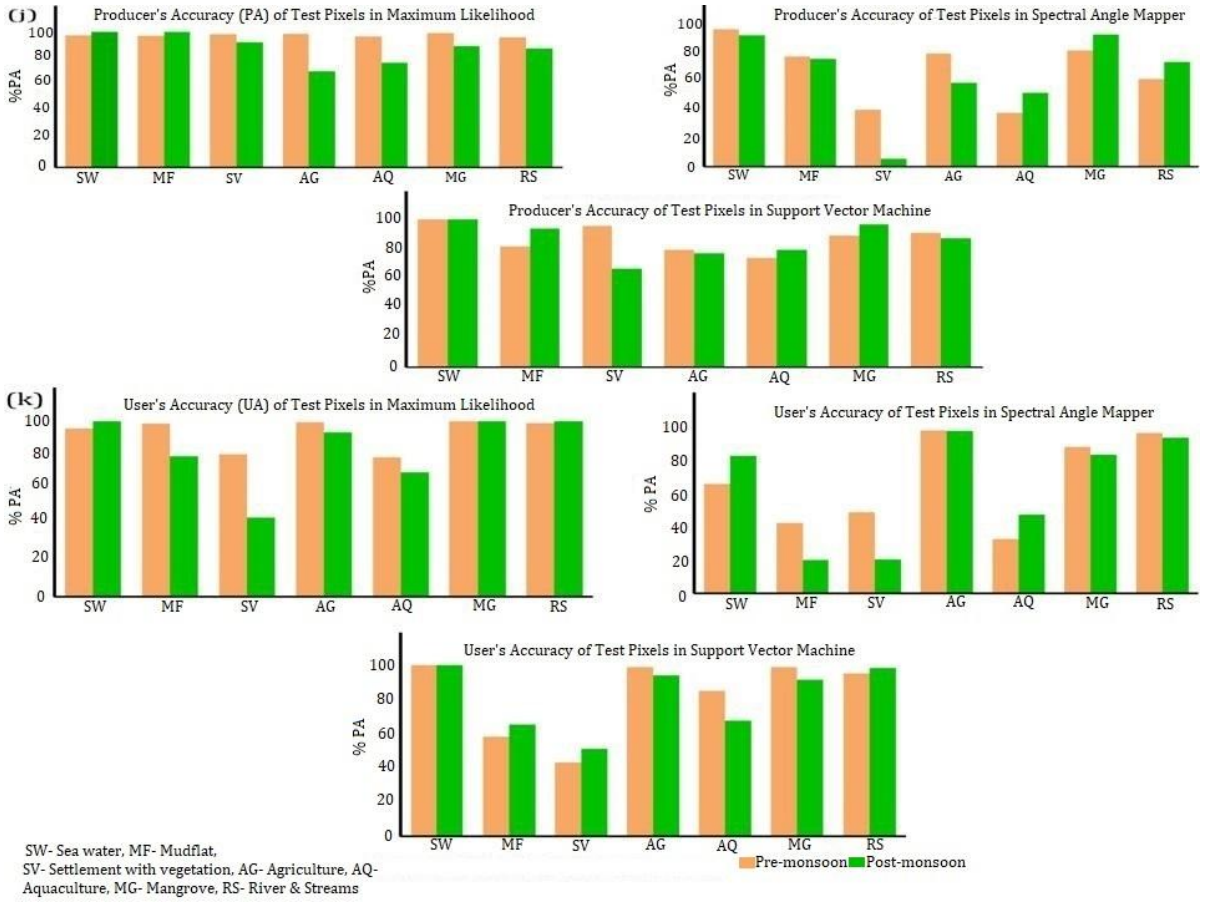

Fig. 6: (j) Producer's Accuracy and (k) User's Accuracy of Test Pixels

Interpretation of Classifier Performance in Seasonal Context

A comparative evaluation of classifiers using AUC-ROC analysis highlights their efficacy in distinguishing LULC classes (Talukdar et al., 2020). ML achieved the highest AUC values (0.98 pre-monsoon, 0.96 post-monsoon), reflecting its superiorityin overcoming spectral overlaps and dynamic environmental conditions. SVM also performed well, with AUC values of 0.82 (pre-monsoon) and 0.81 (post-monsoon), demonstrating its robustness in addressing seasonal spectral variability. SAM, in contrast, exhibited lower AUC values (0.69 pre-monsoon, 0.64 post-monsoon), confirming its limited ability to alleviateinterclass spectral overlaps.

Analyzing the classification accuracy of the individual LULC classes further reveals the effectiveness of the classifiers. During the pre-monsoon season, ML exhibited exceptionally high user's accuracy (UA) for mangroves (100%), settlement with vegetation (81.26%), and mudflats (98.68%),emphasizing its reliability in delineating the different categories(Fig. 6) (Table 3). SVM also showed high UA for mangroves (98.80%) and seawater (100%) (Table 9). In contrast, SAM's performance was hindered by its sensitivity to spectral variations, with lower UA values for settlement with vegetation (48%) and aquaculture (32.14%) (Table 10). In the post-monsoon dataset, ML maintained relatively high UA for mangroves (100%) and agriculture (93.59%), followed by SVM, with 91.49% UA for mangroves and 51.16% UA for settlement with vegetation, respectively(Tables5and 4). However, SAM performed poorly, particularly forsettlements with vegetation (20%) and mudflats (19.64%) (Table 11).

The producer's accuracies (PA) provide additional insights into classifier performance (Fig. 6). In the pre-monsoon dataset, ML achieved a PA of 99.01% for mangroves and 97.33% for seawater (Table 3). SVM also achieved high PA for mangroves (89.13%) and seawater (100%) (Table 9). Conversely, SAM struggled with lower PA values for mangroves (84.71%) and mudflats (80%) (Table 10). During the post-monsoon season, ML maintained high PA for mangroves (89.25%),aquaculture (77.27%), and rivers and streams (87.65%), although these values were lower than those in the pre-monsoon dataset. SVM, however, achieved a PA of 96.63% for mangroves, highlighting its efficacy in overcoming the interclass spectral similarities in post-monsoon conditions (Table 4).The varying performance of these classifiers is attributed to the algorithms they use (Fig. 7). For instance, ML's statistical approach ensures consistent accuracy across varying conditions, while SVM's ability to handle high-dimensional feature spaces results in high classification accuracy across different

categories (Pepper et al., 2022). In contrast, SAM's reliance on spectral angle measurement limits its effectiveness in scenarios with overlapping spectral signatures, such as the post-monsoon period.

Table 9. Accuracy Matrix (in %) of Test Pixels of the Classified Image (LANDSAT 9, APRIL 25, 2024) - SVM Classifier

LULC	SW	RS	MG	MF	AG	SV	AQ	Row Total	UA
SW	11	0	0	0	0	0	0	11	100.00
RS	0	60	0	1	1	0	1	63	95.24
MG	0	0	82	0	1	0	0	83	98.80
MF	0	5	4	18	4	0	0	31	58.06
AG	0	0	1	0	89	0	0	90	98.89
SV	0	0	5	3	16	22	5	51	43.14
AQ	0	1	0	0	1	1	17	20	85.00
Column Total	11	66	92	22	112	23	23	349	0
PA	100	90.91	89.13	81.82	79.46	95.65	73.91	0	85.67

Table 10. Accuracy Matrix (in %) of Test Pixels of the Classified Image (LANDSAT 9, APRIL 25, 2024) - SAM Classifier

LULC	RS	AG	MG	MF	AQ	SV	SW	Row Total	UA
RS	39	0	0	0	2	0	0	41	95.12
AG	0	84	0	0	1	2	0	87	96.55
MG	0	5	72	0	1	5	0	83	86.75
MF	1	3	6	20	8	10	0	48	41.67
AQ	8	1	6	4	9	0	0	28	32.14
SV	0	9	1	1	2	12	0	25	48.00
SW	13	0	0	0	0	0	24	37	64.86
Column Total	61	102	85	25	23	29	24	349	0
PA	63.93	82.35	84.71	80.00	39.13	41.38	100	0	74.50

Table 11. Accuracy Matrix(in %) of Test Pixels of the Classified Image (LANDSAT 8, November 25, 2023) - SAM Classifier

ClassValue	SW	MF	SV	AG	AQ	MG	RS	Row Total	UA
SW	22	0	0	0	1	0	4	27	81.48
MF	0	11	19	22	3	1	0	56	19.64
SV	0	2	2	3	3	0	0	10	20.00
AG	0	0	1	53	0	1	0	55	96.36
AQ	0	1	2	0	14	2	11	30	46.67
MG	0	0	11	9	2	100	0	122	81.97
RS	1	0	0	0	3	0	48	52	92.31
Column Total	23	14	35	87	26	104	63	352	0
PA	95.65	78.57	5.71	60.92	53.85	96.15	76.19	0	71.02

Comparison with Previous Studies

The classification accuracies obtained in this study align well with, and in some cases are better than, those reported in earlier mangrove monitoring research. For instance, the ML classifier in the Sundarbans achieved an Overall Accuracy of 97.54% ($\kappa = 0.96$) during the pre-monsoon. This is much higher than the 85–90% accuracy range reported by Lee and Yeh (2009) for Taiwanese mangroves using ML and NDVI indices. Likewise, our SVM results (OA = 84.7%, $\kappa = 0.81$ post-monsoon) compare well with those of Deval and Joshi (2022), who found SVM to yield 82–86% accuracy in mapping semi-arid wetland vegetation. These parallels support the robustness of SVMs for heterogeneous, seasonally dynamic ecosystems.

The poor performance of SAM in this study (71–74% OA) echoes earlier findings by Kruse et al. (1993) and subsequent applications, which reported its limitations in situations of high interclass spectral similarity. This reinforces the idea that angle-based spectral classifiers are less effective in tropical areas where vegetation and water classes overlap seasonally.

In contrast, studies using more advanced classifiers and higher-resolution data have reported accuracies comparable to or better than those reported here. RF and ANN applied in the Red Sea mangroves achieved >90% OA while improving landscape connectivity (Bindajam et al., 2023). Likewise, Sawant et al. (2024) demonstrated reliable mangrove change detection along the Mumbai coast using CART and RF, achieving classification accuracies over 90%. Zhao et al. (2024) achieved high accuracies in mapping national-scale mangrove species in China with Sentinel-2 imagery combined with machine learning, highlighting the advantages of finer spatial and spectral resolution.

What distinguishes this study is its precise evaluation of seasonal effects on classifier performance using Landsat-8/9 OLI data, an area that has received little focus in previous Sundarbans research. While higher-resolution datasets (e.g., Sentinel-2) enable more precise species-level classification, our results indicate that even with moderate-resolution Landsat data, ML can outperform nonparametric methods when seasonal variability is carefully accounted for. Thus, this study provides an important benchmark for using medium-resolution satellite imagery in dynamic estuarine ecosystems, where seasonal hydrology significantly affects spectral separability.

Table 12: Comparative Accuracy of Classifiers in Previous Studies vs. Present Study

Study/ Location	Dataset	Methods	Reported Accuracy	Present Study (Sundarbans,Landsat- 8/9)
Lee & Yeh (2009), Taiwan	Landsat, NDVI	ML	85–90%	ML = 97.54% (pre-monsoon), 83.71% (post-monsoon)
Deval & Joshi (2022), India	Landsat, Wetlands	SVM	82–86%	SVM = 85.67% (pre), 84.70% (post)
Kruse et al. (1993), Spectral Applications	Imaging Spectrometer	SAM	~70–75% in mixed classes	SAM = 74.49% (pre), 71.02% (post)
Bindajam et al. (2023), Red Sea	Landsat & ML	RF, ANN	>90%	ML exceeded 95% in Sundarbans (pre-monsoon)
Sawant et al. (2024), Mumbai Coast	Sentinel-2	CART, RF	>90%	Comparable to ML, higher than SVM/SAM
Zhao et al. (2024), China	Sentinel-2	ML (species-level)	>90%	Landsat results of this study confirm ML's robustness despite coarser resolution.

Implications for Mangrove Ecosystem Monitoring

These findings have significant implications for the conservation and sustainable management of mangroves in the Indian Sundarban. The superior performance of ML and SVM classifiers underscores their potential for generating high-accuracy LULC maps, which are critical for monitoring mangrove health and assessing the impacts of climate and anthropogenic disturbances (Maurya et al., 2021). The seasonal variations in classifier performance also emphasize the need for temporal analysis to account for ecological and hydrological dynamics (Fig. 7).

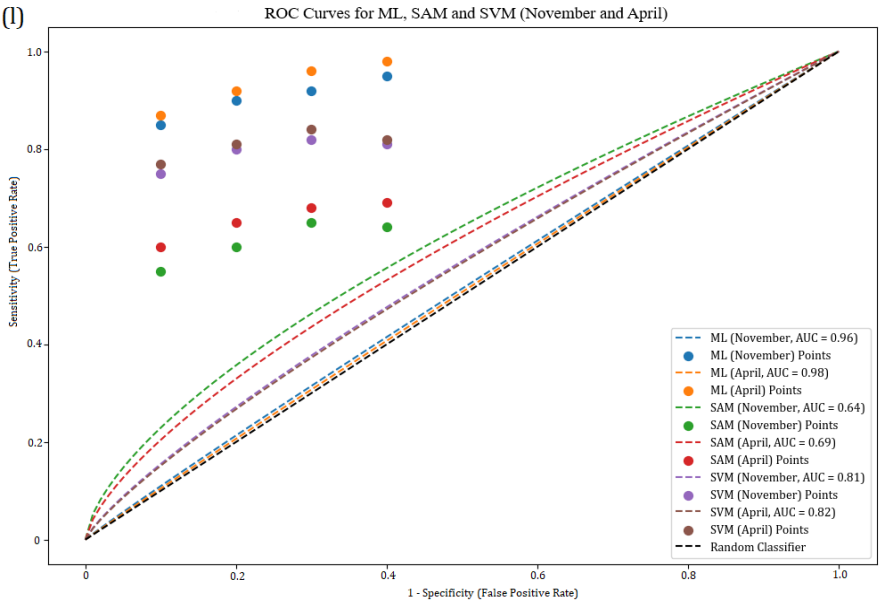

Fig. 7: AUC- ROC Curve

Preprocessed Level-2 Landsat data, corrected for radiometric, geometric, and atmospheric distortions, played a crucial role in enhancing classification accuracy. The consistent satellite pass time at approximately 10:30 AM local time ensured uniform illumination conditions, minimizing spectral reflectance variability. Implementing advanced classifiers demonstrates the potential of remote sensing and machine learning techniques for robust mangrove ecosystem monitoring.

Future Research Directions

Future studies could expand on this research's findings by incorporating hyperspectral data and additional machine learning techniques, such as Random Forest, XGBoost, or deep learning models, to further enhance classification accuracy (Shao et al., 2024). Integrating*in-situ* data for model calibration and validation would also improve the reliability of classification results. Additionally, vulnerability mapping vis-à-vis mangrove health assessments could provide a holistic understanding of ecosystem dynamics and adaptive management strategies to mitigate the impact of climate change and anthropogenic activities (Singh et al., 2019).

Conclusion

This study successfully addressed its objectives: discriminating Sundarban mangroves using Landsat OLI images across pre- and post-monsoon seasons, comparing the performance of different machine learning techniques, and evaluating classifier efficacy using the AUC-ROC curve. Maximum Likelihood (ML) and Support Vector Machine (SVM) outperformed Spectral Angle Mapper (SAM) in terms of classification accuracy, with ML achieving the highest accuracy across both seasons. The AUC-ROC analysis further validated ML as the most effective technique for mangrove delineation, achieving superior AUC values (0.98 pre-monsoon, 0.96 post-monsoon) compared to SVM and SAM. Seasonal analysis underscored the importance of temporal approaches in capturing ecological variations and improving classifier reliability.

This study shows that season-aware remote sensing strategies can significantly improve mangrove monitoring and protection. Pre-monsoon datasets were identified as optimal for classification, providing clear guidance for planning monitoring campaigns. At the same time, reliable discrimination between mangroves and agriculture and settlements provides strong baselines for enforcing coastal land-use regulations and detecting encroachment. The findings demonstrate that even moderate-resolution Landsat data, combined with robust classifiers, can deliver actionable insights for agencies and NGOs with limited resources. Embedding such geospatial tools into conservation policies, climate adaptation frameworks, and SDG-linked strategies can enhance resilience planning. At the same time, their demonstrated reliability highlights the potential for near-real-time monitoring to support rapid response and adaptive management in the Sundarbans and similar ecosystems.

Future investigations could include advanced or hybrid approaches to address the limitations of existing classifiers, thereby supporting sustainable management of mangrove ecosystems.

References

Ahmad, A., &Quegan, S. (2012).Analysis of maximum likelihood classification on multispectral data. *Applied Mathematical Sciences*, 6(129), 6425–6436.

Baviskar, P., & Dhiman, R. (2022).Advancing the spatiotemporal assessment of mangrove ecosystem using machine learning approaches—Case study of a coastal megacity, Mumbai, India. *Authorea Preprints*. https://doi.org/10.1002/essoar.10510134.1

Belgiu, M., &Drăguţ, L. (2016).Random forest in remote sensing: A review of applications and future directions. *ISPRS Journal of Photogrammetry and Remote Sensing*, 114, 24–31. https://doi.org/10.1016/j.isprsjprs.2016.01.011

Bindajam, A. A., Mallick, J., Talukdar, S., Shohan, A. A. A., &Alshayeb, M. J. (2023).Assessment of long-term mangrove distribution using optimised machine learning algorithms and landscape pattern analysis. *Environmental Science and Pollution Research*, 30(29), 73753–73779. https://doi.org/10.1007/s11356-023-27395-2

Chopra, R., Verma, V. K., & Sharma, P. K. (2001).Mapping, monitoring and conservation of Harike wetland ecosystem, Punjab, India, through remote sensing. *International Journal of Remote Sensing*, 22(1), 89–98. https://doi.org/10.1080/014311601750038866

Deval, K., & Joshi, P. K. (2022).Vegetation type and land cover mapping in a semi-arid heterogeneous forested wetland of India: Comparing image classification algorithms. *Environment, Development and Sustainability*, 24(3), 3947–3966. https://doi.org/10.1007/s10668-021-01596-6

Ghosh, A., Mukherjee, S., Sen, N., Dasgupta, M., & Naskar, K. R. (2002).Check-list of mangroves and mangrove associated species in the Indian Sundarbans. *Seshaiyana*, 10(2), 211–224.

Giri, C., Pengra, B., Zhu, Z., Singh, A., & Tieszen, L. L. (2007).Monitoring mangrove forest dynamics of the Sundarbans in Bangladesh and India using multi-temporal satellite data from 1973 to 2000. *Estuarine, Coastal and Shelf Science*, 73(1–2), 91–100. https://doi.org/10.1016/j.ecss.2006.12.019

Heumann, B. W. (2011).An object-based classification of mangroves using a hybrid decision tree—Support vector machine approach. *Remote Sensing*, 3(11), 2440–2460. https://doi.org/10.3390/rs3112440

Islam, M. M., Borgqvist, H., & Kumar, L. (2019).Monitoring mangrove forest land cover changes in the coastline of Bangladesh from 1976 to 2015. *Geocarto International*, 34(13), 1458–1476.

Jensen, J. R. (1996).*Introductory digital image processing: A remote sensing perspective* (2nd ed.). Prentice-Hall Inc.

Keerthi, S. S., DeCoste, D., & Joachims, T. (2005).A modified finite Newton method for fast solution of large scale linear SVMs. *Journal of Machine Learning Research*, 6(3), 341–361.

Kruse, F. A., Lefkoff, A. B., Boardman, J. W., Heidebrecht, K. B., Shapiro, A. T., Barloon, P. J., & Goetz, A. F. H. (1993).The spectral image processing system (SIPS)—Interactive visualization and analysis of imaging spectrometer data. *Remote Sensing of Environment*, 44(2–3), 145–163.

Lee, T. M., & Yeh, H. C. (2009).Applying remote sensing techniques to monitor shifting wetland vegetation: A case study of Danshui River estuary mangrove communities, Taiwan. *Ecological Engineering*, 35(4), 487–496. https://doi.org/10.1016/j.ecoleng.2008.01.007

Liu, X., & Yang, C. (2013).A kernel spectral angle mapper algorithm for remote sensing image classification. In *2013 6th International Congress on Image and Signal Processing (CISP)* (Vol. 2, pp. 814–818). IEEE. https://doi.org/10.1109/CISP.2013.6745277

Maurya, K., Mahajan, S., & Chaube, N. (2021).Remote sensing techniques: Mapping and monitoring of mangrove ecosystem—A review. *Complex & Intelligent Systems*, 7(6), 2797–2818. https://doi.org/10.1007/s40747-021-00457-z

Pepper, N., Crespo, L., &Montomoli, F. (2022). Adaptive learning for reliability analysis using support vector machines. *Reliability Engineering & System Safety*, 226, 108635.

Rajamani, S. K., & Iyer, R. S. (2023). Machine learning-based mobile applications using Python and Scikit-Learn. In *Designing and developing innovative mobile applications* (pp. 282–306). IGI Global. https://doi.org/10.4018/978-1-6684-8582-8.ch016

Sawant, S., Bonala, P., Joshi, A., Shindikar, M., Patil, A., Vyas, S., & Deobagkar, D. (2024). Integration of machine learning and remote sensing for assessing the change detection of mangrove forests along the Mumbai coast. *Journal of Earth System Science*, 133 (4), 186. https://doi.org/10.1007/s12040-024-02378-0

Sen, H. S. (2019).*The Sundarbans: A disaster-prone eco-region*. Berlin: Springer.

Shao, Z., Ahmad, M. N., & Javed, A. (2024). Comparison of Random Forest and XGBoost classifiers using integrated optical and SAR features for mapping urban impervious surface. *Remote Sensing*, 16(4), 665. https://doi.org/10.3390/rs16040665

Singh, P. K., Papageorgiou, K., Chudasama, H., & Papageorgiou, E. I. (2019). Evaluating the effectiveness of climate change adaptations in the world's largest mangrove ecosystem. *Sustainability*, 11(23), 6655. https://doi.org/10.3390/su11236655

Small, C., & Sousa, D. (2024). Spectroscopic phenological characterization of mangrove communities. *Remote Sensing*, 16(15), 2796. https://doi.org/10.3390/rs16152796

Sun, W., Chang, C., & Long, Q. (2019, December). Bayesian non-linear support vector machine for high dimensional data with incorporation of graph information on features. In *2019 IEEE International Conference on Big Data (Big Data)* (pp. 4874–4882). IEEE.

Talukdar, S., Singha, P., Mahato, S., Pal, S., Liou, Y. A., & Rahman, A. (2020). Land-use land-cover classification by machine learning classifiers for satellite observations—A review. *Remote Sensing*, 12(7), 1135. https://doi.org/10.3390/rs12071135

USGS. (2023). Landsat Collection 2 Level-2 Science Products. *U.S. Geological Survey*.https://www.usgs.gov

Zhao, C., Jia, M., Zhang, R., Wang, Z., Ren, C., Mao, D., & Wang, Y. (2024).Mangrove species mapping in coastal China using synthesized Sentinel-2 high-separability images. *Remote Sensing of Environment*, 307, 114151. https://doi.org/10.1016/j.rse.2024.114151